2018 Building Performance Analysis Conference and
SimBuild co-organized by ASHRAE and IBPSA-USA
Chicago, IL
September 26-28, 2018

AEROACOUSTIC FAÇADE NOISE: PREDICTING WIND-INDUCED NOISE FROM PERFORATED FAÇADE PANELS

Nathaniel L Jones and Alexej Goehring
Arup, San Francisco, CA

ABSTRACT

In this paper, we propose a method to quantify the likelihood that perforated exterior façade panels will produce wind-induced noise. This noise is generated by pressure fluctuations when vortices shed off the panels. The frequency and audibility are influenced by panel geometry, wind velocity, turbulence, and wind angle of incidence. We performed parametric computational fluid dynamic (CFD) analyses of perforated panels to calculate sound pressure levels and trained a machine learning algorithm on that data. We applied the learned relationship to a building scale CFD analysis accounting for annual variation of wind direction and strength to predict the likelihood of noise at any location on the building for a typical weather year.

INTRODUCTION

External shading devices are increasingly used as façade elements to meet ever more stringent energy codes. Designs vary from vertical or horizontal fins to perforated metal panels. When such façade elements are installed in wind-prone areas, air passing through perforations or skipping along them can generate unwanted noise. This is especially likely in applications on tall buildings, where panels are exposed to increased wind speeds at high elevations. Recent cases of wind-induced whistling and humming from buildings in Manchester (Hamer, 2006) and Montevideo (Lisboa, et al., 2015) demonstrate the annoyance of the phenomenon and the need to prevent it through predictive analysis.

To calculate the risk of unwanted noise, we must analyze buildings at multiple length and time scales. At the architectural scale, analysis of a façade element can produce a sound level and spectrum associated with vortex shedding under a steady incoming air stream. On the regional scale, climate analysis predicts the frequency of occurrence of wind events. Intermediate to these two scales, computational fluid dynamic (CFD) analysis shows how regional wind conditions translate to local air movement on façade panels.

In this paper, we describe the factors that affect wind-induced noise from perforated façade panels and propose a method to quantify the risk of unwanted noise occurrence (Figure 1). As a case study, we consider a 33-story building proposed for a site in the Pacific Northwest which is to be clad in perforated shading panels. The design may generate noise because of several factors, including pressure fluctuations that result from vortex shedding off the panels. The frequency and audibility are influenced by hole diameter, hole spacing, panel thickness, wind velocity, turbulence intensity, and wind angle of incidence. We created a parametric model of the perforated panel and used CFD to calculate sound power and pressure levels. We trained a machine learning algorithm on that data and applied the learned relationship to a global building scale CFD analysis accounting for climatological statistics of wind strength and directionality to predict the frequency of noise occurrence at any location on the building. Using this method, we predict wind-induced noise levels on the building, the areas that would be most affected by noise, and how often they would generate noise.

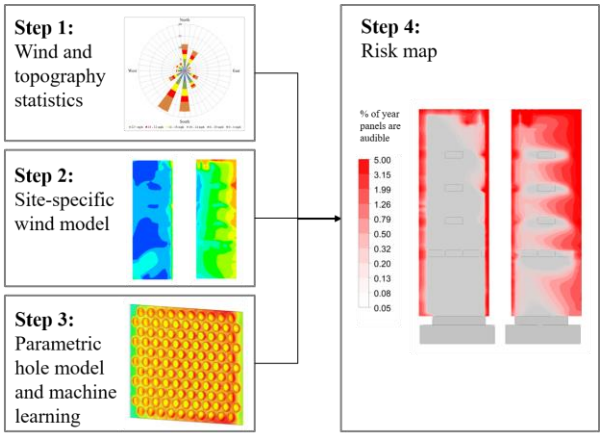

Figure 1 Method for determining noise risk

BACKGROUND

Human Perception of Noise

Sound is the human perception of vibrations traveling through air or another medium. Undesirable sound is called noise. Noise can be characterized by its frequency content (roughly, its pitch) and its loudness. Human perception of noise is highly dependent on these characteristics. The human ear can hear frequencies between 20 and 20,000 Hz but is more sensitive to sounds in the speech frequencies (500 – 5000 Hz) when compared to the lower or upper ranges (Figure 2).

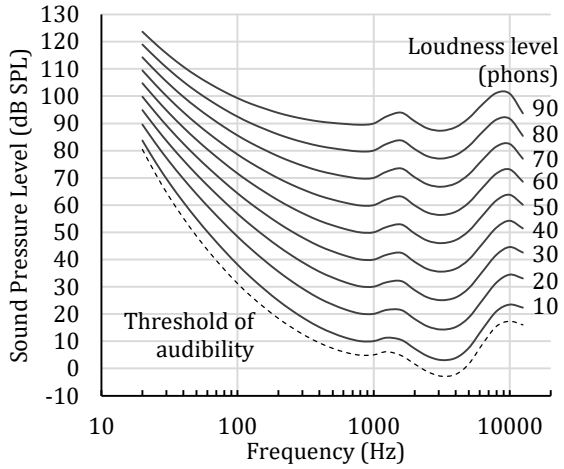

Figure 2 Curves of equal loudness for frequencies audible to humans (after ISO, 2003). We are most sensitive to frequencies between 500 – 5000 Hz.

Audible sounds that include one main frequency, such as a note played on a musical instrument, are called tonal. Sounds which include many frequencies, such as the sound of indoor mechanical systems, are said to be broadband spectral. Tonal noise is often perceived more readily than broadband spectral noise. This is because tonal noise is distinct, whereas broadband noise often blends into the background.

The loudness of a sound source can be described by its sound power P in watts or sound power level SWL in decibels (dB). However, sound radiates from a point source and dissipates in the process. The loudness of noise experienced by an observer can be described by sound pressure p in pascals or sound pressure level SPL in decibels, which corresponds to the actual pressure exerted by the traveling sound wave:

$$P = \frac{Ap^2}{\rho c} cos\,\theta \qquad (1)$$

In this relationship, A is the surface area of a volume enclosing the source, ρ is the density of air, c is the speed of sound, and θ is the angle to the direction of the source.

Aeroacoustic Noise

Several mechanisms allow wind to induce noise in objects. In some mechanisms, the objects themselves are made to vibrate and emit noise as the wind passes by. In other mechanisms, the presence of the object causes oscillations in air pressure which leads to noise.

These mechanisms can be categorized as monopole, dipole, or quadrupole sources. A monopole source uniformly radiates pressure waves into a medium; a fluid inlet with unsteady velocity or an imploding steam bubble acts as a monopole sound source. A dipole source results from unsteady momentum rather than unsteady mass flow; a vibrating plate or fluid boundary acts as a dipole sound source. A quadrupole source results from turbulent flows. Such turbulence occurs when incident wind flow is forced to undergo sharp angle changes within a short distance. This has the potential to generate unsteady pressure fluctuations within the audible range.

When wind encounters elements (in this case, the holes in a perforated panel), vortices arise downwind of the object. Air emerging through a perforation may act as a monopole source, while the downstream vortices act as quadrupole sources. The characteristic frequency of these vortices depends on the size and geometry of the object and the velocity of the wind:

$$f = \frac{U \times St}{D} \qquad (2)$$

Here, f is the frequency of the potential noise generated, U is the incident wind speed, D is the characteristic length (*e.g.* hole diameter or panel thickness), and St is the Strouhal number, a dimensionless value that describes the geometry of the obstacle for a given flow regime. The Strouhal number is between 0.15 and 0.2 for circular perforations for wind speeds considered as part of this study. When f is in the audible frequency range (20 – 20,000 Hz), aeroacoustic noise is generated. Thus, 17-mm-diameter perforations like those common in our study may generate audible noise under wind speeds as low as 2 m/s (4.5 mph).

Numerical Simulation

Computational fluid dynamics (CFD) models flows of liquids and gases by solving the Navier-Stokes equations. This enables the modeling of wind around buildings as well as airflow through perforated panels.

Noise levels can be calculated based on a rearrangement of the Navier-Stokes equations (Lighthill, 1952). In Lighthill's analogy, the Navier-Stokes equations reduce to a wave equation and source terms representing monopoles, dipoles, and quadrupoles. Considering only quadrupole sources and statistical theory of isotropic turbulence, Lighthill's analogy is further rearranged into

the Proudman Broadband Noise model (Proudman, 1952), which relates acoustic power P in W/m^3 to the density of air ρ, eddy dissipation ε, turbulence kinetic energy k, speed of sound c, and a constant ($\alpha = 0.1$):

$$P = \alpha\rho\varepsilon\left(\frac{\sqrt{2k}}{c}\right)^5 \quad (3)$$

Using the Reynolds-averaged Navier-Stokes (RANS) method to solve the fluid field, values for k and ε are readily available from the subgrid scale model. The total sound power P_V in watts generated in a volume V is the volume integral of the result:

$$P_V = \int_V P dV \quad (4)$$

Proudman's model holds for turbulent fluids with low Mach numbers. In RANS simulation, it has previously been used to model the noise generation by automobiles (Ringwall, 2017) and gas jets (ANSYS, 2015).

Alternatively, transient CFD simulations can model pressure waves at various frequencies directly. A common approach is to use large eddy simulations (LES) (Witkowska, et al., 1997). Unlike RANS simulation, LES produces frequency output and sound pressure levels in addition to overall sound power, but it requires small time steps to resolve pressure waves at audible frequencies, making it computationally expensive for parametric testing.

Wind Tunnel Tests

Wind tunnel tests have a long history with aeroacoustic testing. However, despite distinct advantages (*e.g.* the ability to record sound pressures and frequencies), there are also shortcomings due to scale, background noise, and wind speed variability. Previous wind tunnel tests demonstrate that perforated panels generate tone-like as well as broadband noise (Feng, 2012). These tests correspond well with *in situ* measurements (Lisboa, et al., 2015) that recorded wind-induced broadband noise loud enough to be perceived as annoying (ISO, 2007).

METHOD

Wind Conditions at the Project Site

For our analysis, we need a probability distribution of wind speeds and directions at the case study site. In this section, we describe our analysis of local wind records. First, we transposed wind data records from an airport anemometer site to be consistent with the elevation, terrain, and topography of the project's urban location. Then we assessed the frequency of occurrence of the regular winds by strength and direction.

Exposure Correction

We obtained an hourly history of wind data from an airport near the project site and scanned it for data gaps and anomalies. The historic wind records were collected from the National Climate Data Center, which preserves climate and historical weather data gathered by the National Oceanic and Atmospheric Administration (NOAA).

We used the widely accepted Deaves and Harris (1978) log-law wind model of the atmospheric boundary layer to estimate the effect of upwind terrain, as specified by Engineering Sciences Data Unit (ESDU, 2010). We carried out a detailed survey of terrain roughness for the airport weather station using satellite images. The effective height of the anemometer was taken as 10 m (33 ft). We transposed the wind speed history to a surface roughness classified as open-country terrain. This considers the terrain around the anemometer site and converts the measured wind speeds to a comparable reference speed consistent with ASCE 7-10 (2010). The analysis was completed for 30° sectors and up to 40 km (25 miles) from the anemometer site. The surface roughness length z_0 was chosen to be consistent with the model used in ESDU. We repeated the ESDU terrain assessment for the project site, and transposed the wind speeds estimated for open-country to the project site.

Probabilistic Wind Speed

We considered the percent of time each wind direction occurred when determining the overall risk of wind-induced façade noise. We fit Weibull distributions to histograms of wind strength from each of twelve directions at the project site. Each of the twelve Weibull curves forms a wind speed probability distribution, and the areas under the twelve curves together sum to unity. As shown in Figure 3, winds from the southwest and south are strongest and occur most frequently at the site.

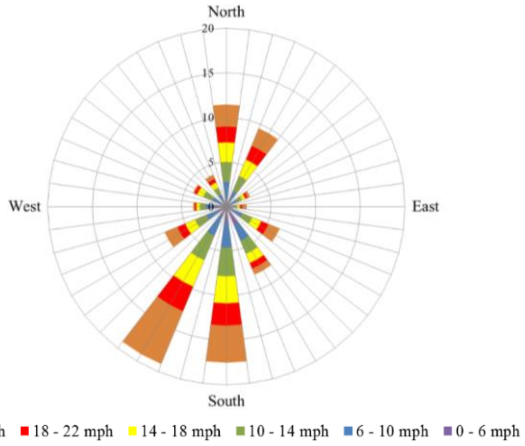

Figure 3 Annual wind rose indicating the direction and strength of winds at project site

Using these wind predictions for the project site, we derived appropriate simulation profiles for the whole-building CFD simulations. These profiles include data on mean and gust wind speed, turbulence intensity, and turbulence length scale for 30° wind sectors (Figure 4).

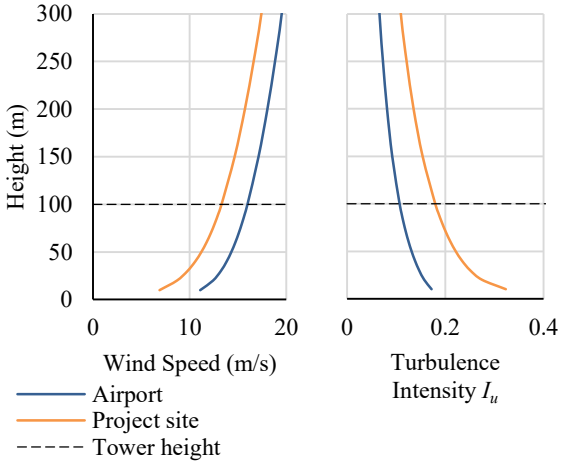

Figure 4 Representative wind speed and turbulence profiles for southerly winds

Aeroacoustic Modeling

In this section, we quantify the likelihood of exceeding certain sound pressure levels at any given point on the façade. First, we calculate how the building and its surroundings modulate wind directionality and increase wind strength. Second, we calculate the noise generation at each panel under varying wind conditions and develop a mathematical relationship using machine learning. The former is an external influencing factor, and the latter is a characteristic of panel geometry.

Whole-Building Simulation

We modeled the case study building and approximately one square mile of the surrounding topography and urban terrain. CFD simulations of this domain allow us to characterize the flow of wind around the project site and the façade of the building. We are particularly interested in the wind speed, direction, and turbulence intensity 20 cm (8 in.) from the façade, the offset distance of the perforated panels. To measure these, we created reference planes at this offset distance from the tower geometry.

We simulated twelve wind directions (at 30° increments) to extract wind accelerations around the building for each oncoming wind direction. Figure 5 and Figure 6 show cross sections through the flow field in which effects of upstream, downstream, and out-of-plane buildings are apparent. We normalize wind speeds by the incoming speed at anemometer height to give wind speed ratios. Figure 7 and Figure 8 illustrate the wind speed ratio and angle of incidence on the reference plane on the north and south façades for the most common southerly wind direction. Corner balcony locations are evident as areas of higher wind speed and head-on angle.

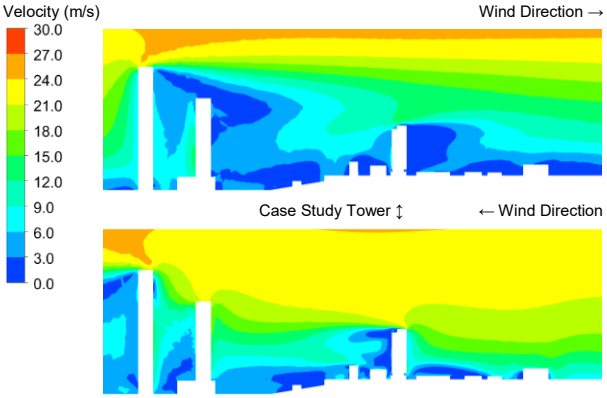

Figure 5 Wind speeds at the project site for two of the twelve wind directions, based on a 10 m/s wind speed at reference height at entry to the domain

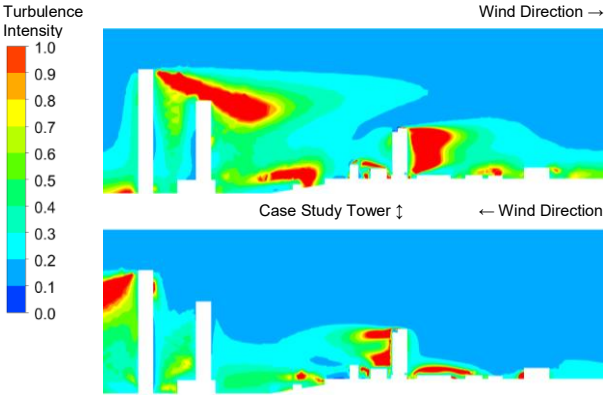

Figure 6 Turbulence intensity at the project site for two of the twelve wind directions

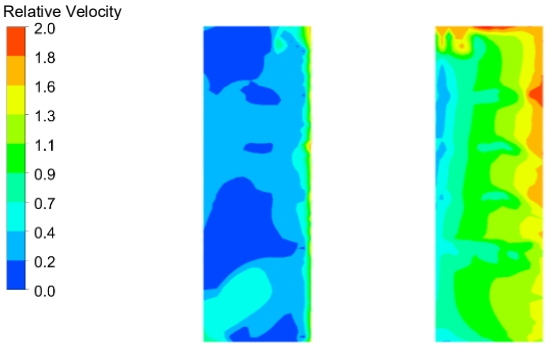

Figure 7 Relative wind speed illustrating accelerations around the west facade corners for the north (left) and south (right) façades, shown for southerly winds

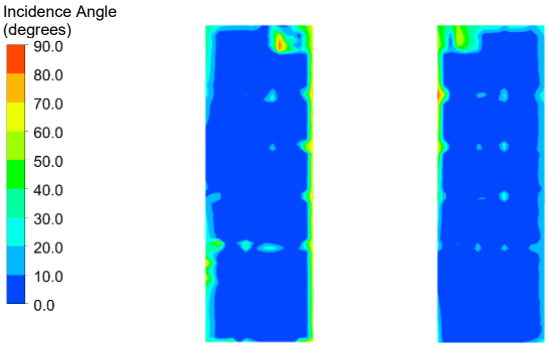

Figure 8 Angle formed between wind direction and panel surface for north (left) and south (right) façades, shown for southerly winds

Parametric Simulation of Noise Generation

We created a parametric model of a 300 mm × 300 mm (1 ft × 1 ft) panel section. The model allowed us to change the hole diameter (from 5 to 34 mm) and hole spacing (from 22 to 44 mm on center). Additionally, we varied three parameters of the air stream in CFD simulation: wind speed (from 5 to 40 m/s), angle of incidence (from 0 to 90°), and turbulence intensity (from 1 to 15%). Note that the panel may generate noise even in the parallel wind condition, as the thickness of the panel at each perforation can shed vortices.

Aeroacoustic noise is generated due to turbulence in the flow field. When the frequency of the fluctuations is within the human perceptive range, these fluctuations become audible. By solving the Reynolds-averaged Navier-Stokes (RANS) equations and using the Proudman Broadband Noise model, we can quantify the total sound power for each case in the parametric model (Figure 9).

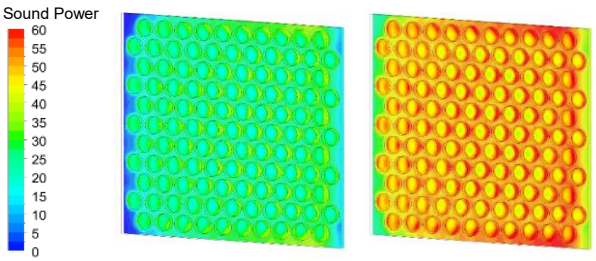

Figure 9 Volumetric sound power level (dB) of a 17mm perforated facade panel for a 5 m/s (left) and 10 m/s (right) wind speeds with wind 30° from normal

By rearranging Equation (1), we convert sound power to sound pressure:

$$p = \sqrt{\frac{P}{A}\frac{\rho c}{\cos\theta}} \tag{5}$$

In our case study, each panel acts as an area source, so we assume the panel and bounding volume have the same surface area and θ equals zero. We therefore write $p = \sqrt{P\rho c}$ and convert to decibels:

$$SPL = 20\,log_{10}\frac{p}{p_0} \tag{6}$$

where the reference sound pressure $p_0 = 2 \times 10^{-5}$ Pa. Up to half the sound generated may escape through the panel to the outside, and some sound may reflect of the building façade, so the actual sound pressure level may be up to 3 dB less than our prediction. We do not consider attenuation through the façade construction or interior noise levels in our analysis, so our prediction of sound pressure levels is only valid in the cavity between the building and panel.

Table 1 shows the effect of the total sound power level (dB) per panel for the most common hole configuration (17 mm diameter and 22 mm spacing) with 1% turbulence intensity. The more perpendicular the flow to the panel, the louder the sound emission for any given wind speed. Similarly, the higher the wind speed, the louder the sound emission.

Table 1 Effects of wind speed and angle of incidence on total sound power level (dB) per panel

WIND SPEED (MPH)	ANGLE OF INCIDENCE				
	15°	30°	45°	60°	75°
25	49	44	37	27	15
50	74	70	62	52	40
75	89	84	77	67	54
100	99	94	87	77	64

Machine Learning of Noise Generation

We ran 71 simulations of the parametric model. Although the parametric simulations cover the range of expected wind conditions on the tower, they do not cover every possible parameter combination. Rather than run an exhaustive set of simulations, we used machine learning to develop a relationship between the model parameters and resulting sound pressure level:

$$SPL = f(U, \theta, I, d, s) \tag{7}$$

Here, the parameters describing the wind incident on the panel are speed U, incidence angle θ, and turbulence intensity I, and the parameters describing the panel geometry are hole diameter d and percent openness s.

We considered multiple machine learning algorithms. We chose polynomial regression over other methods such as artificial neural networks to achieve a solution portable between software tools. We chose second order polynomials because sound pressure levels showed a

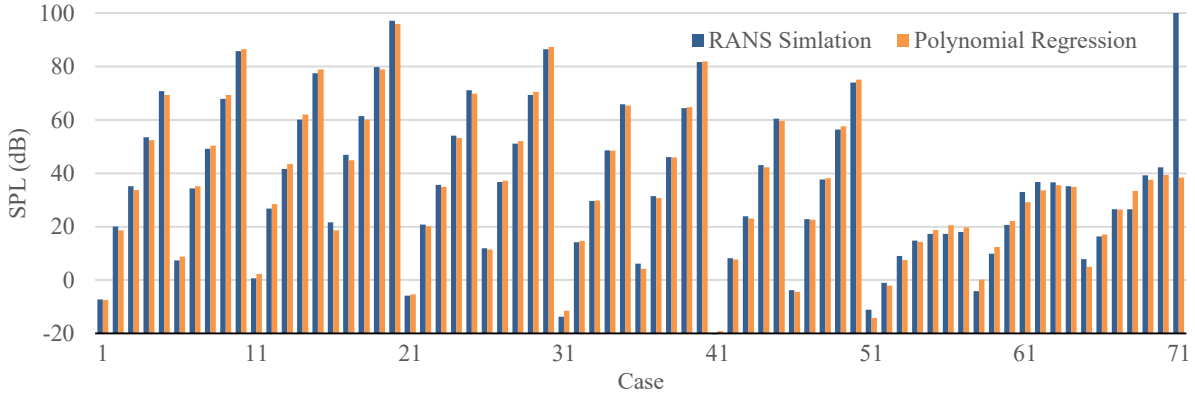

Figure 10 Predicted sound pressure levels from polynomial regression show good correspondence to those from RANS simulation

single maximum around an 11 mm hole diameter. Third order polynomials would have produced a curve of the wrong shape, and fourth order risked overfitting.

To better fit the data, we used the logarithm of wind velocity in our regression model rather than velocity itself (due to the physical relationship of wind power to SPL in decibels). This produced a 99% fit score—a slight improvement over the 98% score achieved otherwise.

Figure 10 shows the sound pressure levels measured from parametric RANS simulation together with the regression fit for the same parameter combinations. In all cases except the last, the prediction is within 7 dB of simulation results, with an average discrepancy of 2 dB. The last case involved normal wind incidence on the least porous panel. In this case, forcing air through small apertures leads to much higher air velocities in the façade cavity than are seen elsewhere. In the building context, resistance from the panel makes this scenario unlikely to occur.

Frequency Content

We computed the frequency content of the wind-induced noise using transient large eddy simulations (LES). These CFD simulations differ from the parametric RANS simulations in that they actively resolve the turbulent fluctuations at any time-step such that velocity fluctuations can be read as pressures waves. Figure 11 illustrates the flow and turbulence through a panel section from the transient simulations. Performing a fast Fourier transform on the pressure fluctuations indicates a resonant frequency in the fluid domain correlated to the Strouhal number for two critical dimensions, hole diameter and hole spacing (Figure 12).

This analysis also identified that the tonal frequency increases as wind is accelerated through the panels, so smaller holes produce more content in audible frequencies.

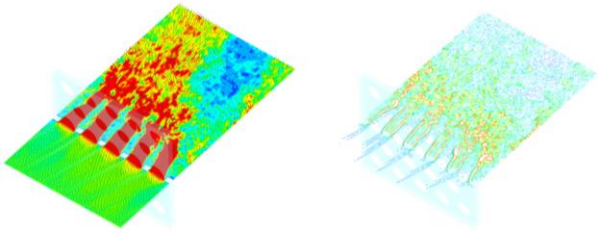

Figure 11 LES simulations show velocity (left) and curl (right) used to derive relationship between total and audible sound power

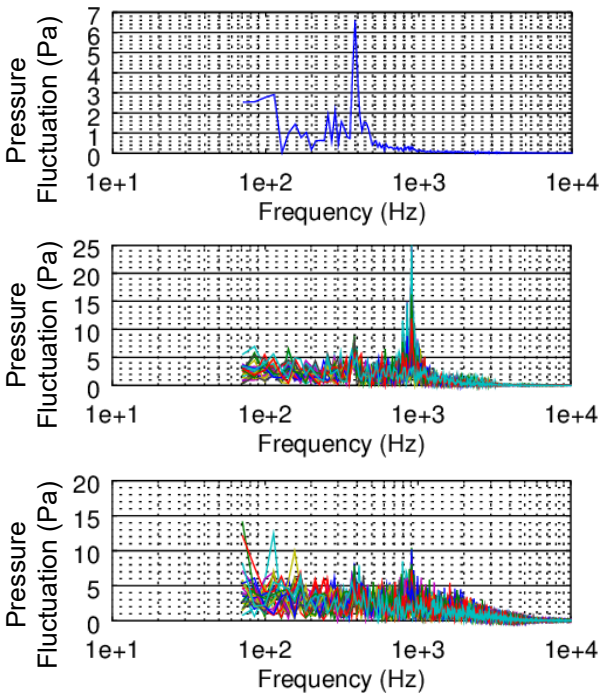

Figure 12 Spectral analysis of pressure fluctuations at boundaries and in the flow field indicating resonant frequencies at 450 Hz and 950 Hz for a 17 mm hole panel at a nominal wind speed of 10 m/s

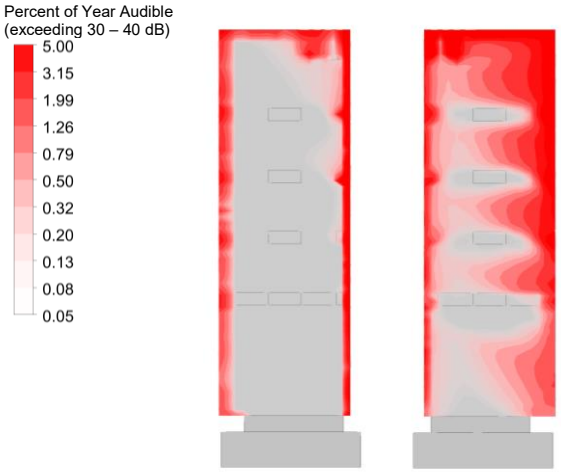

Figure 13 Risk of audible sound pressure levels (exceeding 30 – 40 dB) for the north (left) and south (right) façades of the tower

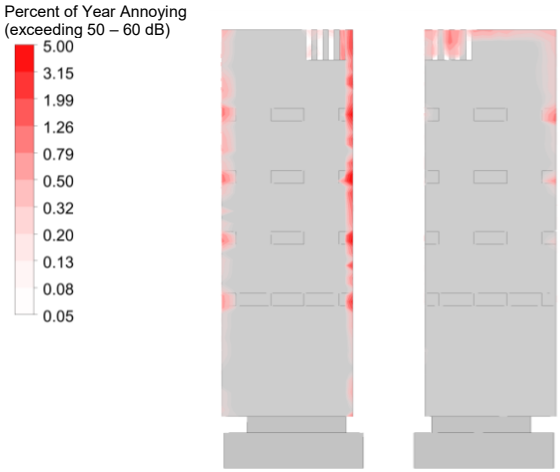

Figure 14 Risk of annoying sound pressure levels (exceeding 50 – 60 dB) for the north (left) and south (right) façades of the tower

Risk Assessment

Combining the site-specific wind study, whole building simulation, and linear regression analysis allows us to quantify the noise level on the façade for any wind condition. For each of the twelve wind directions at each point on the façade, we find incidence angle, turbulence intensity, and perforation size and spacing. Based on the polynomial regression results, we calculate the minimum local wind speed necessary to achieve a minimum sound pressure level. We then determine the fraction of time over all wind directions when the given sound pressure level is exceeded using the Weibull curves. We can therefore calculate the risk of exceeding a given decibel level as a percentage of time occurrence per year at any point on the façade.

The risk of audible noise is not uniform across all façade exposures. Areas near the center of each façade are unlikely to experience high noise generation as the flow of wind is mainly parallel to the façade. However, the building corners and areas near the penthouse, especially on the west façade, are more prone to it. In the case study, areas with greater exposure are likely to generate wind-induced noise for 5% to 10% of the year (see Figure 15 and Figure 16). Variation in wind direction at the site will cause different parts of the tower to exhibit wind induced noise at different times. Areas of the tower shown to be at risk may not be concurrently at risk.

Given the site's proximity to a highway, ambient noise will mask some wind-induced noise. To interpret the risk and choose appropriate mitigation steps, the sound emitted from a panel needs to be placed in context with background noise, sound reflection, absorption, and reverberations due to the building geometry. This context may justify setting a high minimum sound pressure level for risk calculation.

Note that other noise sources may contribute to the overall aeroacoustic noise level. Our study does not consider wind-induced vibrations of the panels or their fastening hardware.

CONCLUSION

We performed a risk assessment reviewing the likelihood of wind-induced noise originating from perforated façade panels by:

- Assessing site specific wind conditions, including probabilities of wind directions and wind speeds.
- Modelling the wind accelerations and wind directionality around the case study building.
- Simulating aeroacoustic noise generation based on geometric and wind condition parameters and fitting a polynomial regression model to the results.

We combined these three methods to map the risk of aeroacoustic noise audibility spatially on the façade of the case study building.

The assessment found that the corners and top of the building are most prone to wind-induced noise. Sound pressure levels of 50 – 60 dB are expected to be exceeded for 5 – 10% of the year, which in a typical urban setting would be audible. Higher sound pressure levels may occur and will be less frequent.

This study demonstrates that building performance simulation can detect wind-induced noise risk from architectural cladding before problems arise. In the

future, similar risk assessments should also consider the propagation and perception of noise inside the building as well as site-specific background noise measurement. This ability we described is useful for predicting aeroacoustic phenomena generally and will have increasing importance as new digital manufacturing techniques make acoustic-scale façade patterns more widely available.

ACKNOWLEDGMENT

The authors sincerely thank the team that lent their expertise to this project. Melissa Burton, Adam Jaffe, and Rubina Ramponi carried out portions of the wind study. Steven Downie lent critical insights to the aeroacoustic modeling. Iraklis Koutrouvelis provided guidance on machine learning.

REFERENCES

ANSYS, Inc., 2015. *Summary: Modeling acoustics of a coaxial jet using broadband noise model,* Cheyenne, Wyoming: SAS IP, Inc.

ASCE, 2010. *Minimum design loads for buildings and other structures. ASCE/SEI 7-10.* Reston, Virginia: American Society of Civil Engineers.

Deaves, D. M. & Harris, R. I., 1978. *A Mathematical model of the structure of strong winds. Report 76.* London: Construction Industry Research and Information Association.

ESDU 01008c, 2010. *Computer program for wind speeds and turbulence properties: Flat or hilly sites in terrain with roughness changes,* London: IHS Engineering Sciences Data Unit.

Feng, L., 2012. Tone-like signal in the wind-induced noise of perforated plates. *Acta Acustica united with Acustica,* 98(1), pp. 188-194.

Hamer, M., 2006. Buildings that whistle in the wind. *New Scientist*, 2 August.

ISO, 2003. *Acoustics—Normal equal-loudness-level contours. ISO 226:2003.* Geneva: International Organization for Standardization.

ISO, 2007. *Acoustics—Description, measurement and assessment of environmental noise—Part 2: Determination of sound pressure levels. ISO 1996-2:2007,* Geneva: International Organization for Standardization.

Lighthill, M. J., 1952. On sound generated aerodynamically I. General Theory. *Proceedings of the Royal Society. Series A, Mathematical and Physical,* 211(107), pp. 564-587.

Lisboa, M. R., Ottieri, J. C. & González, A. E., 2015. Noise annoyance due to wind flow interaction with a building's facade. *Open Journal of Acoustics,* Volume 5, pp. 1-10.

Proudman, I., 1952. The generation of noise by isotropic turbulence. *Proceedings of the Royal Society. Series A, Mathematical and Physical,* 214(1116), pp. 119-132.

Ringwall, E., 2017. *Aeroacoustic sound sources around the wheels of a passenger car—A Computational Fluid Dynamics study using steady state models to evaluate main sources of flow noise,* Master's thesis: Chalmers University of Technology.

Witkowska, A., Juvé, D. & Brasseur, J. G., 1997. Numerical study of noise from isotropic turbulence. *Journal of Computational Acoustics,* 5(3), pp. 317-336.